Identifying the intermittent flow sub-regimes using pressure drop time series fluctuations

Abderraouf Arabi (arabi.abderraouf@sonatrach.dz)
Sonatrach, Direction Centrale Recherche et Développement https://orcid.org/0000-0002-3581-5416
Yacine salhi
University of Sciences and Technology Houari Boumediene USTHB, Physics' Faculty Laboratory of Theoretical and Applied Fluid Mechanics, LMFTA https://orcid.org/0000-0003-3218-8135
Youcef Zenati
University of Sciences and Technology Houari Boumediene USTHB, Physics' Faculty Laboratory of Theoretical and Applied Fluid Mechanics, LMFTA https://orcid.org/0000-0002-6389-625X
El-Khider Si-Ahmed
Nantes Université https://orcid.org/0000-0002-5556-6314
Jack Legrand
Nantes Université https://orcid.org/0000-0001-9028-7575

Research Article

Keywords: Gas-liquid two-phase flow, Intermittent gas-liquid flow, Sub-regimes, Pressure drop time series fluctuations, PDF, Statistical parameters

Posted Date: January 25th, 2023

DOI: https://doi.org/10.21203/rs.3.rs-2510593/v1

Abstract

From a literature survey, it has been noticed a lack of objective methods to identify and distinct between the intermittent flow sub-regimes. Thus, the aim of this study is to analyze pressure drop fluctuations using statistical methods in order to propose simple tools to characterize the sub-regimes of the intermittent flow. The pressure drop time series were collected from experiments carried out using air-water mixture and 30 mm ID pipe. The utilization of transparent pipes allowed to identify three sub-regimes which are Plug flow, Less Aerated Slug flow (LAS flow), and Highly Aerated Slug flow (HAS flow). It was found that the PDF displayed a unimodal distribution in all cases studied. Meanwhile, the representation of the base width and maximum values of PDF as function of the gas-to-liquid superficial velocities ratio and the mixture Froude number, respectively, showed that the points for each sub-regime are clustered in the same zone. So, these two feature spaces can be used to identify the sub-regimes. A third feature space, based on the statistical parameters standard deviation and kurtosis, was also proposed as a tool to distinguish between the three sub-regimes.

1 Introduction

In many industrial installations, a gas and a liquid can flow together. For instance, in the oil and gas industry (Kiran et al., 2020) or in chemical reactors (Wang et al., 2021), where several types of fluids are encountered. Moreover, a phase change caused by evaporation or condensation may induce the appearance of a second one in a pipe. Such phenomena occur mainly in petroleum and gas production and in nuclear reactors (Sassi et al., 2020).

It is important to identify and control the flow pattern for a better design and control of the industrial devices (Raeiszadeh et al., 2018). Under certain conditions, the liquid and gas phases may flow alternately and irregularly as elongated bubble (also called gas pocket or gas slug) and bulk of liquid regions filling the entire pipe as liquid slug (Mohmmed et al., 2021, Liu et al., 2022), resulting in the intermittence of flow parameters such as pressure, void fraction, flow rates of both phases, heat and mass coefficients, etc. This flow regime, called intermittent flow, represents a destructive flow pattern (Saini et al., 2022; Adouni et al., 2022), which makes it challenging for the engineers. Indeed, the alternating flow of the two structures causes several industrial problems such as instability of heat and mass exchange in chemical reactors and liquid overflow in upstream installations. To date, the exact nature of the intermittent flows is not yet well known (Mohmmed et al., 2021). Subdividing the intermittent regime into sub-regimes may be a way to better understand and comprehend this type of flow, especially from the aspect of fluid-structure interaction (Arabi et al., 2020d). Based on the shape of the elongated bubble/liquid slug interface and the aeration of the slugs, Thaker and Banerjee (2015, 2016a) proposed to classify the intermittent flow into three sub-regimes:

- Plug flow (Fig. 1.a): In this flow sub-regime, the liquid slugs are free from gas bubbles. The elongated bubble has a staircase shape tail with a hydraulic jump followed by a long tail.

- Less Aerated Slug flow (LAS flow) (Fig. 1.b): The transition from plug flow to slug flow is accompanied by the presence of gas bubbles inside the liquid slugs. In LAS flow, the liquid slugs transport small quantities of gas bubbles. The elongated bubbles end by a simple hydraulic jump without a presence of the long tail.
- Highly Aerated Slug flow (HAS flow) (Fig. 1.c): Comparatively to LAS flow, the liquid slugs in the case of HAS flow carried out large quantities of gas bubbles. The presence of eddies due to the secondary flow represents also a criterion used to differentiate the HAS flow from LAS flow.

Our group has obtained interesting results using this classification approach in series of recent works. Indeed, it was found that the slug frequency (Arabi et al., 2020), the pressure drop (Arabi et al., 2021c) and the behaviour of the flow structures crossing a sudden expansion (Arabi et al., 2021d), depend on the nature of the sub-regime. Despite these results, the investigations carried out using these sub-regimes classification are still scarce, as indicated by the limited number of existing flow pattern maps, showing the zones of the existence of these sub-regimes (Thaker and Banerjee, 2016; Dinaryanto et al., 2018; Humami et al., 2018).

As mentioned earlier, this approach to classify sub-regimes, as well as flow regimes (Arabi et al., 2022), is based on visual observations. This technique of identifying and distinguishing between regimes and sub-regimes is restricted to transparent pipes. As recently reminded by Arabi et al. (2022), various devices for measuring different flow parameters such as static pressure (Drahoš et al., 1987; Luo et al, 2010; Hanafizadeh et al., 2016), differential pressure between two points in the pipe (pressure drop) (Luo et al., 2010; Arabi et al., 2018), void fraction (Kong et al., 2018; Bouyahiaoui et al., 2020), liquid holdup (Deendarlianto et al., 2019; Arellano et al., 2020), velocity (Wang et al., 2020; Xu et al., 2020) and temperature (Guo et al., 2020) have been used to characterize the flows and in particular to identify the flow regimes. Temporal fluctuations of flow parameters in two-phase flows (except for the case of smooth stratified flow) do not allow considering the averaged parameters as reliable data. Excluding the fluctuating components of these parameters does not reflect the physical reality of the phenomena (Wang and Shoji, 2002), especially in case of intermittent flows where fluctuations are the most important. The analysis of time series signal fluctuations is done either through signal visualization (Weismann et al., 1979; Dinaryanto et al., 2018; Arabi et al., 2018; Ma et al., 2020), or by using statistical tools, notably statistical moments (Kadji et al., 2009; Zeghloul et al., 2017) and the Probability Density Function (PDF) (Drahoš and Čermák, 1989; Amani et al., 2020). It should be observed that frequency analysis has also been used (Wang and Shoji, 2002; Arabi et al., 2018). Utilization of more sophisticated analysis techniques was also reported in the literature (see for instance the reviews carried out recently by Saini and Banerjee (2021) and Wijayanta et al. (2022)). The PDF obtained from void fraction or liquid holdup series is frequently used as a tool to identify the regimes (Costigan and Whalley, 1997; Parsi et al., 2017; Abdulkadir et al., 2020a, 2020b). Indeed, each regime has its own PDF shape. The transitions between the regimes can also be detected by an abrupt change in some parameters' values (Bertola, 2003). Ye and Guo (2013) have extracted different statistical parameters and principal components from pressure signals in order to propose a tool for identifying the flow patterns in pipeline-riser systems. By

applying different feature space, which designates the plot of the collected data using the calculated parameters as coordinates, the authors have found that the data of each regime are clustered in separate region. It is important to note that the feature space is not widely used to study two-phase flow in straight pipe. Abdulkadir et al. (2018) used it by plotting the mixture velocity versus the measured mean void fraction values. The authors reported that this feature space can be used as a flow pattern map for both horizontal and vertical pipes. By plotting the slug frequency data using the gas based Strouhal number as function of the mixture Froude number, Arabi et al. (2020) proposed this feature space as a tool to distinguish between the sub-regimes of the intermittent flow.

Among the most common flow monitoring devices in the industry, the absolute and differential pressure transducer have several advantages: robust, easy to use, non-intrusive and inexpensive (Arabi et al., 2020; Wu et al., 2022). Weismann et al. (1979) used pressure drop signals between two points in a pipe for the flow regimes identification in horizontal configuration. They observed that the signal for each flow regime is characterized by its own signature. The signal is smooth for the stratified regime, and contains low amplitude peaks for the wavy flow. For the slug regime, the signal is composed of large peaks with high amplitudes, indicative of the passage of slugs. Indeed, the differential pressure values oscillate with the frequency of liquid slug (Kim and Kim, 2022). The absolute pressure sensor can also be used to detect the passage of liquid slugs (Lin and Hanratty, 1987a; Saini and Banerjee, 2021; Thaker et al., 2021). Wambsganss et al. (1994) plotted the static pressure Root Mean Square (RMS) parameter as function of the mass quality. The authors found that such representation can predict the plug-bubble/slug flow and slug/annular flow transitions well.

By applying the PDF on absolute and differential pressure signals collected from a 50 mm ID horizontal pipe, Luo et al. (2010) found that the PDF of the pressure drop signals had a unimodal profile in case of slug flow while those obtained from the absolute pressure drop signals could have a unimodal or bimodal distribution. They also found that an increase in phasic superficial velocity leads to an increase in the maximum pressure drop, in the maximum pressure and the dispersion of the values collected with the two kinds of signals. It should be noted that the authors observed that the peaks, indicative of the passage of the slugs, were more pronounced in case of differential pressure signals than those obtained with the absolute pressure sensor. This is due to the fact that the former type of sensor filters out the original fluctuations from outside the interval between the two points connected to the pressure sensors (Arabi et al., 2020). Wang et al. (2019) were able to correlate the fluctuations of the pressure drop signals with the void fraction for the bubbly, plug and slug flow regimes. The authors applied the Extreme-Point Symmetric Mode Decomposition (ESMD) components on differential pressure signals collected across a venturi placed on a 40 mm ID horizontal pipe.

Regarding the studies on time series analysis carried out with the sub-regimes of the intermittent flow, Dinaryanto et al. (2018) analyzed the fluctuations of the absolute pressure signals collected on a 16 mm pipe. In the slug and plug flow (which is a transition between plug and LAS flow (Thaker and Banerjee, 2015; Arabi et al., 2021a)), the pressure signals are characterized by small and low fluctuations. The values given by the signals as well as the fluctuations are larger in case of LAS flow. The HAS flow is

characterized by the largest static pressure values and the largest fluctuations. In this study, the authors studied qualitatively the pressure signals for each sub-regime. No quantitative criteria were proposed to distinguish between the sub-regimes. Saini and Banerjee (2021) explained that absolute pressure signals cannot be used as a means of distinguishing between plug, LAS and HAS flows. They proposed to apply the recurrence analysis to these signals. This method is based on the reconstructed phase space trajectory representing non-linear signals from the system in d-dimensional space. From signals obtained using air-water and 25 mm ID pipe, the authors have reported that the recurrence plot and quantification parameters change as the flow transits from one to another sub-regime.

Despite the interesting results obtained by Saini and Banerjee (2021) using the above-mentioned quantitative method, the level of complexity of the latter makes it difficult to be applied on an industrial scale. The present study investigates the fluctuations of the differential pressure time series using simple statistical parameters, such as PDF and statistical moments. The aim of this paper is to propose simple and objective tools to identify and distinct between the sub-regimes of the intermittent flow. The originality of this work resides also in the use of feature space using the parameters obtained from calculated statistical moments and PDF. This paper is a continuation of our works on plug, LAS and HAS flow sub-regimes observed in a 30 mm ID pipe (Arabi, 2019; Arabi et al., 2020b, 2021b, 2021c).

2 Experimental Setup

To carry out this study, a series of pressure drop acquisitions were made using an experimental setup designed to reproduce the stratified, wavy and intermittent gas-liquid flow on horizontal pipes. The diagram of the experimental setup is given in Fig.2. A mixture of air and water were used to generate a gas-liquid two-phase flow. The water and air circulate in close and open circuit, respectively. The flow rates of each phase were measured and injected into a 30 mm ID and 13 m length pipe. An ultrasonic flowmeter and rotameter were used to measure the flow rates of water and air, respectively.

This study concerns the sub-regimes plug, LAS and HAS flows. The sub-regimes were identified from direct observations of the flows through the transparent pipe. The observations are made at a distance of 5.5 m from the input mixer.

The differential pressure transducer is placed to record the pressure drop between points located at 5.2 and 5.8 m from the input mixer. For the detail of the uncertainty associated with the instrumentation used, the readers can be oriented to the refs. (Arabi, 2019; Arabi et al., 2020, 2021b). For each flow pair of superficial velocities, a signal of 30 s duration was sampled with a frequency of 500 Hz. In order to choose the signal duration, the evolution of the mean pressure drop and the standard deviation was plotted as function of the signal duration (Fig. 3) for different values of gas superficial velocity (V_{SG}) and for liquid superficial velocity (V_{SL}) equals to 0.354 m/s. From Fig. 3, it appears that starting from a sampling duration of 20 s, the signal duration has no influence on the mean and standard deviation. The sampling frequency was chosen on the basis of the Power Spectral Density (PSD) spectrum (Fig. 4). We

can see clearly from this frequency analysis that the PSD is distributed in the frequency band below 10 Hz; which indicates that the sampling frequency of 500 Hz is largely sufficient.

3 Results And Discussion

3.1 Flow map

In the present study, a total of 90 visual observations and signal acquisitions were made. The flow conditions, for each sub-regime observed, are plotted in Fig.5 using the superficial velocities of both phases as coordinates. It appears that the transitions between the three sub-regimes depend only on the gas superficial velocity in the experimental conditions studied. Indeed, it was found the presence of plug flow for the case of $V_{SG} \leq 0.786$ m/s. The LAS flow is observed for the intermediate values of gas superficial velocities, while the HAS flow was reported for $V_{SG} \geq 2.35$ m/s. For the authors best knowledge, the LAS/HAS flow transition is reported for the first time in such large pipe. In fact, the existing flow pattern maps of Dinaryanto et al. (2018), Thaker and Banerjee (2016) and Humami et al. (2018) were obtained using a 16, 25 and 26 mm ID pipes, respectively.

3.2 Pressure drop signals

In Fig. 6, we have represented the pressure drop gradient signal collected for V_{SL} = 0.212 m/s and for different gas superficial velocities and sub-regimes. In Plug flow (Figs. 6. a and b), we can observe that the signal is composed of fluctuations, characterizing the alternating passage of liquid slugs and gas pockets in the space between the two pressure taps. The increase of the gas superficial velocities induces a transition to LAS flow. The signal in case of slug flow is also composed of peaks as reported by Weismann et al. (1979), Luo et al., (2010), Arabi et al., (2018, 2020) and Duan et al. (2022). Meanwhile, the amplitudes of signal peaks are more important in the former. With the transition to HAS flow, the amplitude of peaks also increases, which is triggered by the strong aeration of the liquid slugs. The observation of the signals represented in Fig. 6 showed also that an increase of V_{SG} induces an increment of the amplitude of the peaks, which induces a raise of maxima and minima pressure drop gradient recorded values. Thus, the dispersion of values collected for each signal increases.

Figures 7 and 8 display the signals collected for different gas superficial velocities and for V_{SL} equal to 0.354 and 0.778 m/s, respectively. The same behavior reported in the case of V_{SL} = 0.212 m/s was observed: An increment of gas superficial velocity induces an increase of the maximum and minimum pressure drop collected. The latter provokes a rise of the dispersion of the values collected in each signal. The comparison between the signals displayed in Figs. 6.a, 7.a and 8.a (V_{SG} = 0.436 m/s), Figs. 6.b, 7.b and 8.b (V_{SG} = 0.786 m/s), Figs. 6.c, 7.c et 8.c (V_{SG} = 1.179 m/s), Figs. 6.d, 7.d et 8.d (V_{SG} = 1.965 m/s), Figs 6.e, 7.e and 8.e (V_{SG} = 2.751 m/s) and Figs. 6.f, 7.f and 8.f (V_{SG} = 3.537 m/s) shows that an increase of the liquid superficial velocity causes a rise of the peak's number, demonstrating the increase of the slug frequency, which is in adequacy with the observation reported in the works dedicated to the study of this parameter (Thaker and Banerjee, 2016; Arabi et al., 2020; Abdul-Majeed et al., 2021a; Sassi et al.,

2022). The comparison between the figures showed also that the increase of V_{SL}, as V_{GS}, provokes an increase of the absolute values of the maxima and minimum of pressure drop collected.

3.3 PDF

The Probability Density Functions (PDF) of a time series signal parameter expresses the frequency occurrence, expressed in %, of a parameter value in a time series. As mentioned in the section 1, the PDF extracted from void fraction or liquid holdup time series is generally used to identify the flow patterns. Abdulkadir et al. (2018) found that the void fraction's PDF of plug and slug flow have different shape. Indeed, the PDF exhibits two peaks in the latter, while the PDF has a single peak followed by a broadening tail in the plug flow. Using the same kind of signal, Fossa (2001) plotted the maximum values of each PDF obtained as function of the gas superficial velocity. The plug-to-slug flow transition is detected by the occurrence of the maximum of the maxima values of the PDF.

The calculated PDF from the signals collected for V_{SL} = 0.212 m/s are represented in Fig. 9. Qualitative examination of the PDFs obtained in case of plug flow shows that small peak, with a value of ≈ 3.5-6%, is apparent. The PDF, in these cases, is distinguished by a small base width, due to the small amplitude of the differential pressure signals in case of plug flow, as reported in section 3.2. With the transition to the slug flow (LAS and HAS flows combined), we can see in Fig. 9 the increase of a peak in the PDF. The unimodal distribution of the PDF characterizes the slug regime, as suggested by Luo et al. (2010). The increase of the gas superficial velocity leads also to a broadening of the base of the PDF. This is due to an increase of maximum and minimum values of pressure drop values collected, as also reported in section 3.2.

A comparison between the PDF displayed in Figs. 9, 10 and 11 demonstrates that an increase of the liquid superficial velocity induces a flattening of the PDF's, with an increase of their base width and a decrease of the values of maximum of the PDF collected. It was also concluded that the shape of the PDF obtained using pressure drop signals cannot be used to identify the sub-regimes.

We have plotted the base width of the PDF as function of the gas-to-liquid superficial velocities ratio (V_{SG}/ V_{SL}) and the maximum values of the PDF collected for each signal as function of the mixture Froude number $\left(Fr_M = \sqrt{\frac{\rho_L}{\rho_L - \rho_G}} \frac{V_M}{\sqrt{gD}}\right)$ in Fig. 12.a and Fig. 12.b, respectively. V_M refers to the mixture velocity, which is the sum of the gas and liquid superficial velocities ($V_M = V_{SG} + V_{SL}$). We can observe, from Fig. 12.a, that the PDF base width is more important in the HAS flow than in the LAS flow, which in turn are larger than in the plug flow regime. It appears from the two plots that the points for each sub-regime are grouped in the same zone, indicating that these feature spaces can be used as a tool to distinguish between plug, LAS and HAS flows. The obtained flow transition lines between plug and LAS flows and LAS and HAS flows are drawn by solid and dashed lines, respectively. The interesting results observed with the two feature spaces indicate that the mixture Froude number and the gas-to-liquid superficial velocities ratio play a role on the plug-to-LAS flows and LAS-to-HAS flows transitions. Arabi et

al. (2021a) have highlighted the influence of these two dimensionless number on the transition from plug to slug flow.

3.4 Statistical parameters

Figures 13a, 13.b and 13.c show the variation of standard deviation (*Std*), skewness (*Skw*) and kurtosis (*Kur*) as a function of gas superficial velocity for different liquid superficial velocities. The detail of calculation of the three statistical parameters are given in the Appendix. The vertical solid and hatched lines represent the plug/LAS and LAS/HAS flows transitions, respectively. It is clear, from Fig. 13.a, that an increase in the gas superficial velocity induces an increase in the standard deviation, regardless the liquid superficial velocity. This last observation was reported by Luo et al. (2010) in a straight pipe and by Arabi et al. (2018, 2021d) at the upstream of a sudden expansion. One should note that as the liquid superficial velocity increases, the gradient of the variation of the standard deviation as a function of V_{SG} increases. The same behavior was reported by Luo et al. (2010). Moreover, for $V_{SL} \leq 0.283$ m/s, the standard deviation starts to decrease for $V_{SG} \approx 3.0$ m/s, before experiencing an increase. This can be explained by the appearance of pseudo-slugs (Arabi et al., 2018), which occur by the penetration of the gas phase into liquid slugs, and therefore, the pseudo-slugs do not completely bridge the pipe cross-section (Abdul-Majeed et al., 2021b). The latter appears for high gas phase flow rates and low liquid phase superficial velocities as reported by Ruder and Hanratty (1987b), Deendarlianto et al. (2019) and Fan et al. (2022). It should be noted that there are few studies in the literature that have focused on areas where liquid slugs and pseudo-slugs are present simultaneously. Exception for the detection of the presence of the pseudo slugs, it appears that the standard deviation cannot be used as tool to detect the nature of the sub-regimes. The increase of the liquid superficial velocity leads also to an increase of this parameter, as also previously reported by Luo et al. (2010).

Concerning the statistical moments skewness and kurtosis, it seems that an increase in the gas phase flow rate leads to an increase in the values of both statistical parameters. However, with the transition to the HAS flow, the values of the skewness and kurtosis decrease in the case of high liquid superficial velocities.

Finally, we have plotted a feature space using the standard deviation and the kurtosis as coordinates in Fig. 14. This figure shows that the level of the standard deviation is significant of each sub-regime, higher for HAS flow, less for LAS and lower for plug flow. Similar to Figs. 12.a and 12.b, the points for each sub-regime are clustered in the same zone, so we can state that this type of representation can be used as a flow map to differentiate between the three sub-regimes observed. The solid and dashed lines represent the transitions between the plug and LAS flow and between LAS and HAS flows, respectively. It would be interesting to include other data, obtained using other pipe diameters and other fluids, to confirm the validity of this flow chart for further conditions.

4 Conclusions

The purpose of this work is to study the pressure drop signals fluctuations in order to characterize the sub-regimes of intermittent flow. Therefore, a series of pressure drop acquisitions were made in a 30 mm ID horizontal pipe for three sub-regimes: Plug, LAS and HAS flows. The time signals of differential pressure were studied qualitatively and quantitatively using statistical tools. The main conclusions can be summarized as follows:

- For the conditions studied, it was found that only the gas superficial velocity plays a role in the transition of the observed sub-regimes. Indeed, Plug/LAS and LAS/HAS flows transitions were achieved for constant values of V_{SG}.

- The shape of PDF for the cases studied was characterized by a unimodal distribution. Meanwhile, the representation of the base width of the PDF as function of the ratio gas-to-liquid superficial velocities and maximum values of PDF as function of the mixture Froude number can be used as flow map to identify the three sub-regimes.

- Despite the nature of the sub-regime, an increase in phasic superficial velocities increased the absolute values of the standard deviation of the pressure drop.

- The apparition of pseudo-slugs induces a variation of the standard deviation.

- Depictions of the results using as coordinates the kurtosis and standard deviation showed that this type of representation can also be used as a feature space to characterize the three sub-regimes studied. Regarding the three feature spaces proposed, it is important to add additional data obtained with other flow conditions to validate them or to correct the flow transitions.

Declarations

Acknowledgements

The development of two-phase flow test rig used for the present research is supported by the project SONATRACH-U.S.T.H.B. (project number: SH-U.S.T.H.B. RD N °1).

Authors would like to acknowledge the General Direction of Research and Development Technologies/Ministry of Higher Education and Research Sciences DGRSDT/MERS (ALGERIA) for their support.

Declaration of competing interest

The authors have no competing interests to declare that are relevant to the content of this article.

References

1. Abdulkadir, M., Hernandez-Perez, V., Kwatia, C. A., & Azzopardi, B. J. (2018). Interrogating flow development and phase distribution in vertical and horizontal pipes using advanced instrumentation. Chemical Engineering Science, 186, 152-167.
2. Abdulkadir, M., Jatto, D. G., Abdulkareem, L. A., & Zhao, D. (2020a). Pressure drop, void fraction and flow pattern of vertical air–silicone oil flows using differential pressure transducer and advanced instrumentation. Chemical Engineering Research and Design, 159, 262-277.
3. Abdulkadir, M., Zhao, D., Abdulkareem, L. A., Asikolaye, N. O., & Hernandez-Perez, V. (2020b). Insights into the transition from plug to slug flow in a horizontal pipe: An experimental study. Chemical Engineering Research and Design, 163, 85-95.
4. Abdul-Majeed, G. H., Al-Dunainawi, Y., Soto-Cortes, G., & Al-Sudani, J. A. (2021a). Neural Network Model To Predict Slug Frequency of Low-Viscosity Two-Phase Flow. SPE Journal, 26(03), 1290-1301.
5. Abdul-Majeed, G. H., Arabi, A., & Soto-Cortes, G. (2021b). Empirical Correlations for Prediction Slug Liquid Holdup on Slug-Pseudo-Slug and Slug-Churn Transitions in Vertical and Inclined Two-Phase Flow. SPE Production & Operations, 36(03), 721-733.
6. Adouni, H., Chouari, Y., Bournot, H., Kriaa, W., & Mhiri, H. (2022). A novel ventilation method to prevent obstruction phenomenon within sewer networks. International Journal of Heat and Mass Transfer, 184, 122335.
7. Amani, P., Hurter, S., Rudolph, V., & Firouzi, M. (2020). Comparison of flow dynamics of air-water flows with foam flows in vertical pipes. Experimental Thermal and Fluid Science, 119, 110216.
8. Arabi, A. (2019). Contribution à l'étude du comportement d'un écoulement diphasique dans une conduite en présence d'une singularité, Doctoral dissertation, USTHB, Algiers, Algeria.
9. Arabi, A., Azzi, A., Kadi, R., Al-Sarkhi, A., & Hewakandamby, B. (2021a). Empirical Modelization of Intermittent Gas/Liquid Flow Hydrodynamic Parameters: The Importance of Distinguishing between Plug and Slug Flows. SPE Production & Operations, 36(03), 703-720.
10. Arabi, A., Saidj, F., Al-Sarkhi, A., & Azzi, A. (2022). Analogy between Vertical Upward Cap Bubble and Horizontal Plug Flow. SPE Journal, 1-20. https://doi.org/10.2118/209235-PA. (Article in Press).
11. Arabi, A., Salhi, Y., Bouderbal, A., Zenati, Y., Si-Ahmed, E. K., & Legrand, J. (2021b). Onset of intermittent flow: Visualization of flow structures. Oil & Gas Science and Technology–Revue d'IFP Energies Nouvelles, 76, 27.
12. Arabi, A., Salhi, Y., Si-Ahmed, E. K., & Legrand, J. (2018). Influence of a sudden expansion on slug flow characteristics in a horizontal two-phase flow: a pressure drop fluctuations analysis. Meccanica, 53(13), 3321-3338.
13. Arabi, A., Salhi, Y., Zenati, Y., Si-Ahmed, E. K., & Legrand, J. (2020). On gas-liquid intermittent flow in a horizontal pipe: Influence of sub-regime on slug frequency. Chemical Engineering Science, 211, 115251.
14. Arabi, A., Salhi, Y., Zenati, Y., Si-Ahmed, E. K., & Legrand, J. (2021c). A Discussion on the Relation Between the Intermittent Flow Sub-Regimes and the Frictional Pressure Drop. International Journal of Heat and Mass Transfer, 181, 121895.

15. Arabi, A., Salhi, Y., Zenati, Y., Si-Ahmed, E. K., & Legrand, J. (2021d). Experimental investigation of sudden expansion's influence on the hydrodynamic behavior of different sub-regimes of intermittent flow. Journal of Petroleum Science and Engineering, 205, 108834.
16. Arellano, Y., Hunt, A., Haas, O., & Ma, L. (2020). On the life and habits of gas-core slugs: Characterisation of an intermittent horizontal two-phase flow. Journal of Natural Gas Science and Engineering, 82, 103475.
17. Bertola, V. (2003). Experimental characterization of gas–liquid intermittent subregimes by phase density function measurements. Experiments in fluids, 34(1), 122-129.
18. Bouyahiaoui, H., Azzi, A., Zeghloul, A., Hasan, A. H., Al-Sarkhi, A., & Parsi, M. (2020). Vertical upward and downward churn flow: Similarities and differences. Journal of Natural Gas Science and Engineering, 73, 103080.
19. Costigan, G., & Whalley, P. B. (1997). Slug flow regime identification from dynamic void fraction measurements in vertical air-water flows. International Journal of Multiphase Flow, 23(2), 263-282.
20. Deendarlianto, Rahmandhika, A., Widyatama, A., Dinaryanto, O., & Widyaparaga, A. (2019). Experimental study on the hydrodynamic behavior of gas-liquid air-water two-phase flow near the transition to slug flow in horizontal pipes. International Journal of Heat and Mass Transfer, 130, 187-203.
21. Dinaryanto, O., Widyatama, A., Prestinawati, M., Indarto, & Deendarlianto. (2018, August). The characteristics of the sub regime of slug flow in 16 mm horizontal pipe. In AIP Conference Proceedings (Vol. 2001, No. 1, p. 030008). AIP Publishing LLC.
22. Drahoš, J., & Čermák, J. (1989). Diagnostics of gas—liquid flow patterns in chemical engineering systems. Chemical Engineering and Processing: Process Intensification, 26(2), 147-164.
23. Drahoš, J., Čermák, J., Selucký, K., & Ebner, L. (1987). Characterization of hydrodynamic regimes in horizontal two-phase flow: Part II: Analysis of wall pressure fluctuations. Chemical Engineering and Processing: Process Intensification, 22(1), 45-52.
24. Duan, J., Liu, H., Tao, J., Shen, T. A., Hua, W., & Guan, J. (2022). Experimental Study on Gas–Liquid Interface Evolution during Liquid Displaced by Gas of Mobile Pipeline. Energies, 15(7), 2489.
25. Fan, Y., Soedarmo, A., Pereyra, E., & Sarica, C. (2022). A comprehensive review of pseudo-slug flow. Journal of Petroleum Science and Engineering, 110879.Fossa, M. (2001). Gas-liquid distribution in the developing region of horizontal intermittent flows. J. Fluids Eng., 123(1), 71-80.
26. Guo, W., Wang, L., & Liu, C. (2020). Thermal diffusion response to gas–liquid slug flow and its application in measurement. International Journal of Heat and Mass Transfer, 159, 120065.
27. Hanafizadeh, P., Eshraghi, J., Taklifi, A., & Ghanbarzadeh, S. (2016). Experimental identification of flow regimes in gas–liquid two phase flow in a vertical pipe. Meccanica, 51(8), 1771-1782.
28. Humami, F., Dinaryanto, O., Hudaya, A. Z., Widyatama, A., Indarto, & Deendarlianto. (2018, August). Experimental study on the characteristics of flow pattern transitions of air-water two-phase flow in a horizontal pipe. In AIP Conference Proceedings (Vol. 2001, No. 1, p. 030005). AIP Publishing LLC.

29. Kaji, R., Azzopardi, B. J., & Lucas, D. (2009). Investigation of flow development of co-current gas–liquid vertical slug flow. International Journal of Multiphase Flow, 35(4), 335-348.
30. Kim, H. G., & Kim, S. M. (2022). Experimental investigation of flow and pressure drop characteristics of air-oil slug flow in a horizontal tube. International Journal of Heat and Mass Transfer, 183, 122063.
31. Kiran, R., Ahmed, R., & Salehi, S. (2020). Experiments and CFD modelling for two phase flow in a vertical annulus. Chemical Engineering Research and Design, 153, 201-211.
32. Kong, R., Rau, A., Kim, S., Bajorek, S., Tien, K., & Hoxie, C. (2018). Experimental study of horizontal air-water plug-to-slug transition flow in different pipe sizes. International Journal of Heat and Mass Transfer, 123, 1005-1020.
33. Lin, P. Y., & Hanratty, T. J. (1987a). Detection of slug flow from pressure measurements. International Journal of Multiphase Flow, 13(1), 13-21.
34. Lin, P. Y., & Hanratty, T. J. (1987b). Effect of pipe diameter on flow patterns for air-water flow in horizontal pipes. International journal of multiphase flow, 13(4), 549-563.
35. Liu, A., Cheng, L, Yan, C., Gu, H., Meng, Z. (2022). Experimental study on length, liquid film thickness and pressure drop of slug flow in horizontal narrow rectangular channel. Chemical Engineering Research and Design. (Article in Press).
36. Luo, X. M., He, L. M., & Lu, Y. L. (2010, March). Fluctuation characteristics of gas-liquid two-phase slug flow in horizontal pipeline. In AIP Conference Proceedings (Vol. 1207, No. 1, pp. 162-171). American Institute of Physics.
37. Ma, L., He, L., Luo, X., Mi, X., Xu, Y., & Li, Q. (2020). Experimental investigation of gas-liquid two-phase splitting in parallel pipelines with risers. Chemical Engineering Research and Design, 161, 159-167.
38. Mohmmed, A. O., Al-Kayiem, H. H., & Osman, A. B. (2021). Investigations on the slug two-phase flow in horizontal pipes: Past, presents, and future directives. Chemical Engineering Science, 238, 116611.
39. Parsi, M., Azzopardi, B. J., Al-Sarkhi, A., Kesana, N. R., Vieira, R. E., Torres, C. F., ... & Hampel, U. (2017). Do huge waves exist in horizontal gas-liquid pipe flow?. International Journal of Multiphase Flow, 96, 1-23.
40. Raeiszadeh, F., Hajidavalloo, E., Behbahaninejad, M., & Hanafizadeh, P. (2018). Modeling and simulation of downward vertical two-phase flow with pipe rotation. Chemical Engineering Research and Design, 137, 10-19.
41. Saini, S., & Banerjee, J. (2021). Recurrence analysis of pressure signals for identification of intermittent flow sub-regimes. Journal of Petroleum Science and Engineering, 204, 108758.
42. Saini, S., Thaker, J., & Banerjee, J. (2022). Analysis of interfacial dynamics in stratified and wavy-stratified flow using laser Doppler velocimetry. Experimental and Computational Multiphase Flow, 4(2), 142-155.
43. Sassi, P., Fernandez, G., Stiriba, Y., & Pallarès, J. (2022). Effect of solid particles on the slug frequency, velocity and length of intermittent gas-liquid two-phase flows in horizontal pipelines. International Journal of Multiphase Flow, 103985.

44. Sassi, P., Pallarès, J., & Stiriba, Y. (2020). Visualization and measurement of two-phase flows in horizontal pipelines. Experimental and Computational Multiphase Flow, 2(1), 41-51.
45. Thaker, J., & Banerjee, J. (2015). Characterization of two-phase slug flow sub-regimes using flow visualization. Journal of Petroleum Science and Engineering, 135, 561-576.
46. Thaker, J., & Banerjee, J. (2016). Influence of intermittent flow sub-patterns on erosion-corrosion in horizontal pipe. Journal of Petroleum Science and Engineering, 145, 298-320.
47. Thaker, J., Saini, S., & Banerjee, J. (2021). On instantaneous pressure surges and time averaged pressure drop in intermittent regime of two-phase flow. Journal of Petroleum Science and Engineering, 108971.
48. Wambsganss, M. W., Jendrzejczyk, J. A., & France, D. M. (1994). Determination and characteristics of the transition to two-phase slug flow in small horizontal channels.
49. Wang, S. Q., Xu, K. W., & Kim, H. B. (2020). Slug flow identification using ultrasound Doppler velocimetry. International Journal of Heat and Mass Transfer, 148, 119004.
50. Wang, S., & Shoji, M. (2002). Fluctuation characteristics of two-phase flow splitting at a vertical impacting T-junction. International journal of multiphase flow, 28(12), 2007-2016.
51. Wang, W., Liang, X., Zhang, M., & Sefiane, K. (2019). A new method for voidage correlation of gas-liquid mixture based on differential pressure fluctuation. Chemical Engineering Science, 193, 15-26.
52. Wang, X., Li, H., Dong, J., Wu, J., & Tu, J. Y. (2021). Numerical study on mixing flow behavior in gas-liquid ejector. Experimental and Computational Multiphase Flow, 3(2), 108-112.
53. Weisman, J., Duncan, D. G. J. C. T., Gibson, J., & Crawford, T. (1979). Effects of fluid properties and pipe diameter on two-phase flow patterns in horizontal lines. International Journal of Multiphase Flow, 5(6), 437-462.
54. Wijayanta, S., Catrawedarma, I. G. N. B., & Hudaya, A. Z. (2022). Statistical characterization of the interfacial behavior of the sub-regimes in gas-liquid stratified two-phase flow in a horizontal pipe. Flow Measurement and Instrumentation, 102107.
55. Wu, K., Galli, F., de Tommaso, J., Patience, G.S., van Ommen, J.R. (2022). Experimental methods in chemical engineering: Pressure. The Canadian Journal of Chemical Engineering. (Article in press).
56. Xu, K. W., Zhang, Y., Liu, D., Azman, A. N., & Kim, H. B. (2020). Slug flow development study in a horizontal pipe using particle image velocimetry. International Journal of Heat and Mass Transfer, 162, 120267.
57. Zeghloul, A., Azzi, A., Hasan, A., & Azzopardi, B. J. (2018). Behavior and pressure drop of an upwardly two-phase flow through multi-hole orifices. Proceedings of the Institution of Mechanical Engineers, Part C: Journal of Mechanical Engineering Science, 232(18), 3281-3299.

Figures

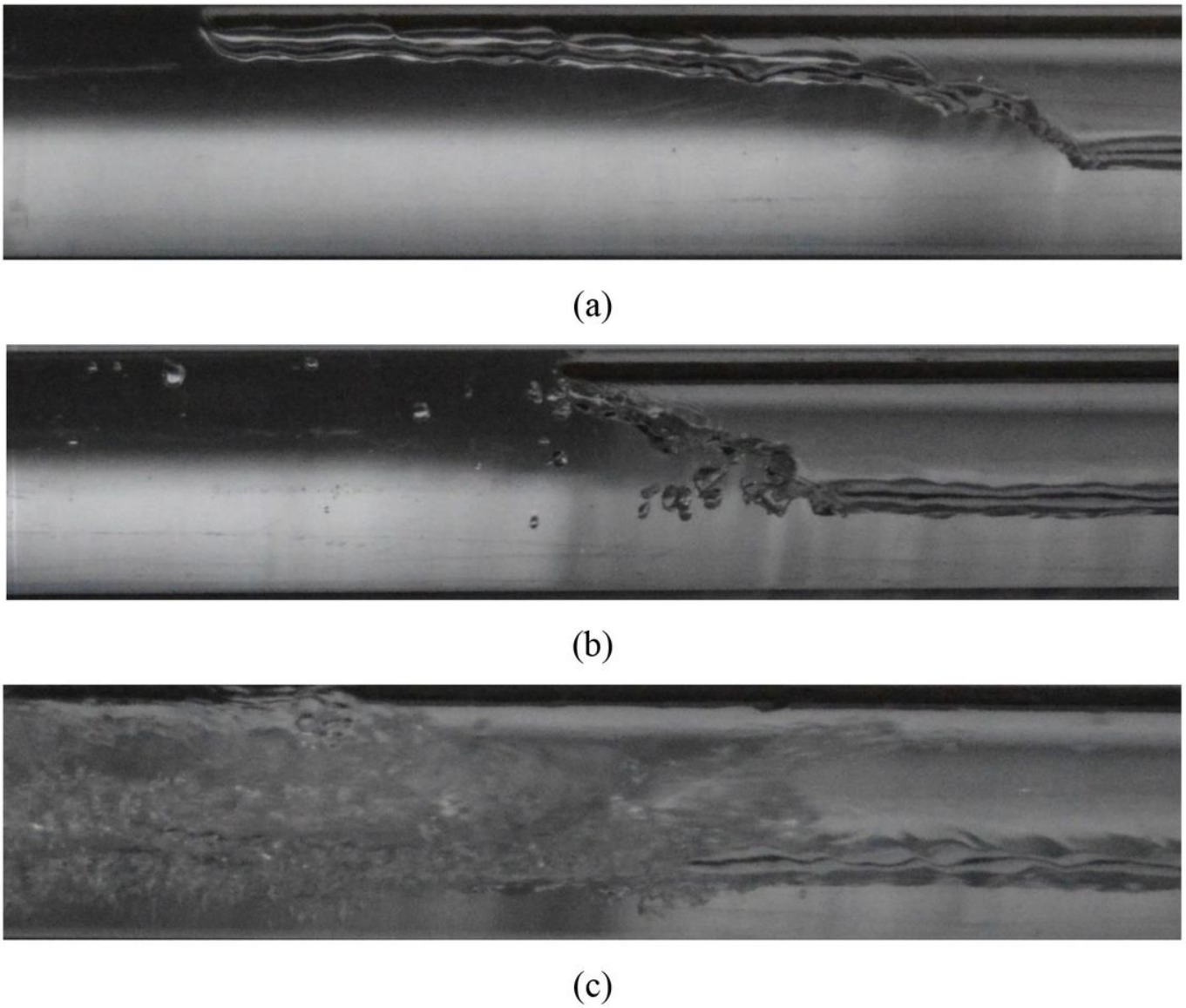

Figure 1

Images of (a) Plug flow; (b) LAS flow and (c) HAS flow observed using a 30 mm ID pipe and air-water mixture. Reprinted from International Journal of Heat and Mass Transfer, vol. 181, Abderraouf Arabi, Yacine Salhi, Youcef Zenati, El-Khider Si-Ahmed, Jack Legrand, A Discussion on the Relation Between the Intermittent Flow Sub-Regimes and the Frictional Pressure Drop, 121895, copyright 2021, with permission from Elsevier.

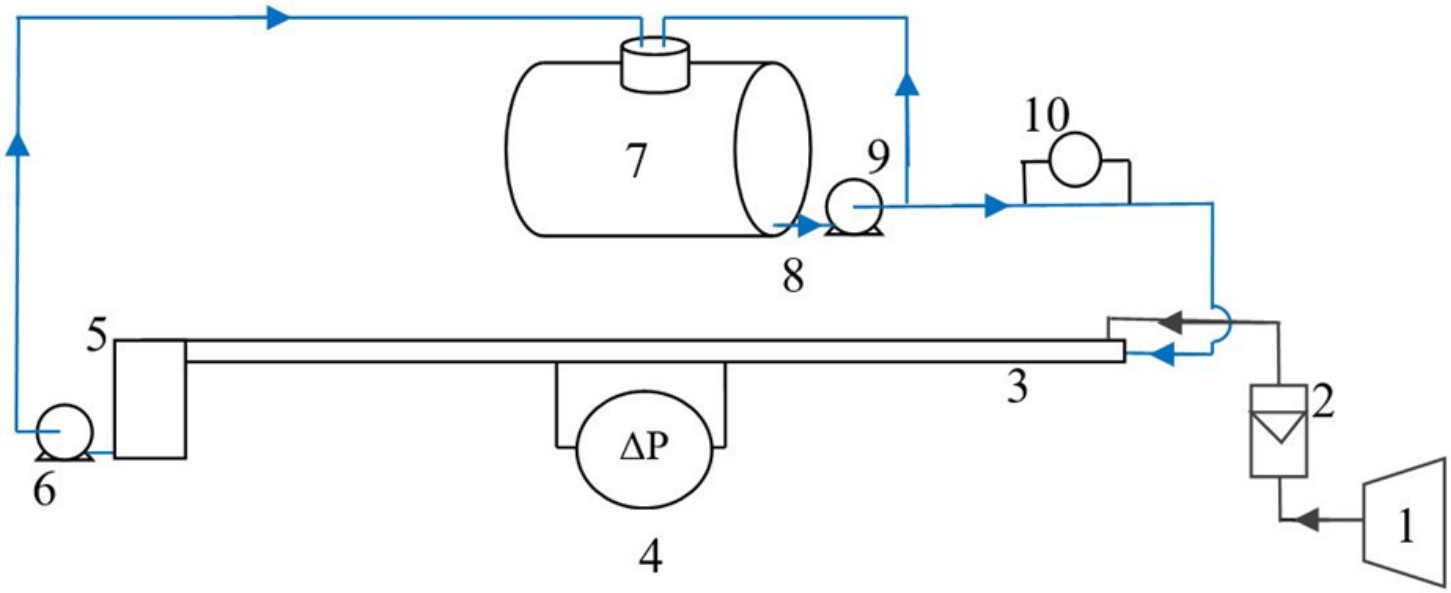

Figure 2

Diagram of the experimental setup used. (1): compressor; (2): air rotameter; (3): 30 mm ID pipe; (4): Differential pressure transducer; (5): decantation tank; (6): pump; (7): liquid tank; (8): Pump; (9): By-pass; (10): ultrasonic liquid flow meter.

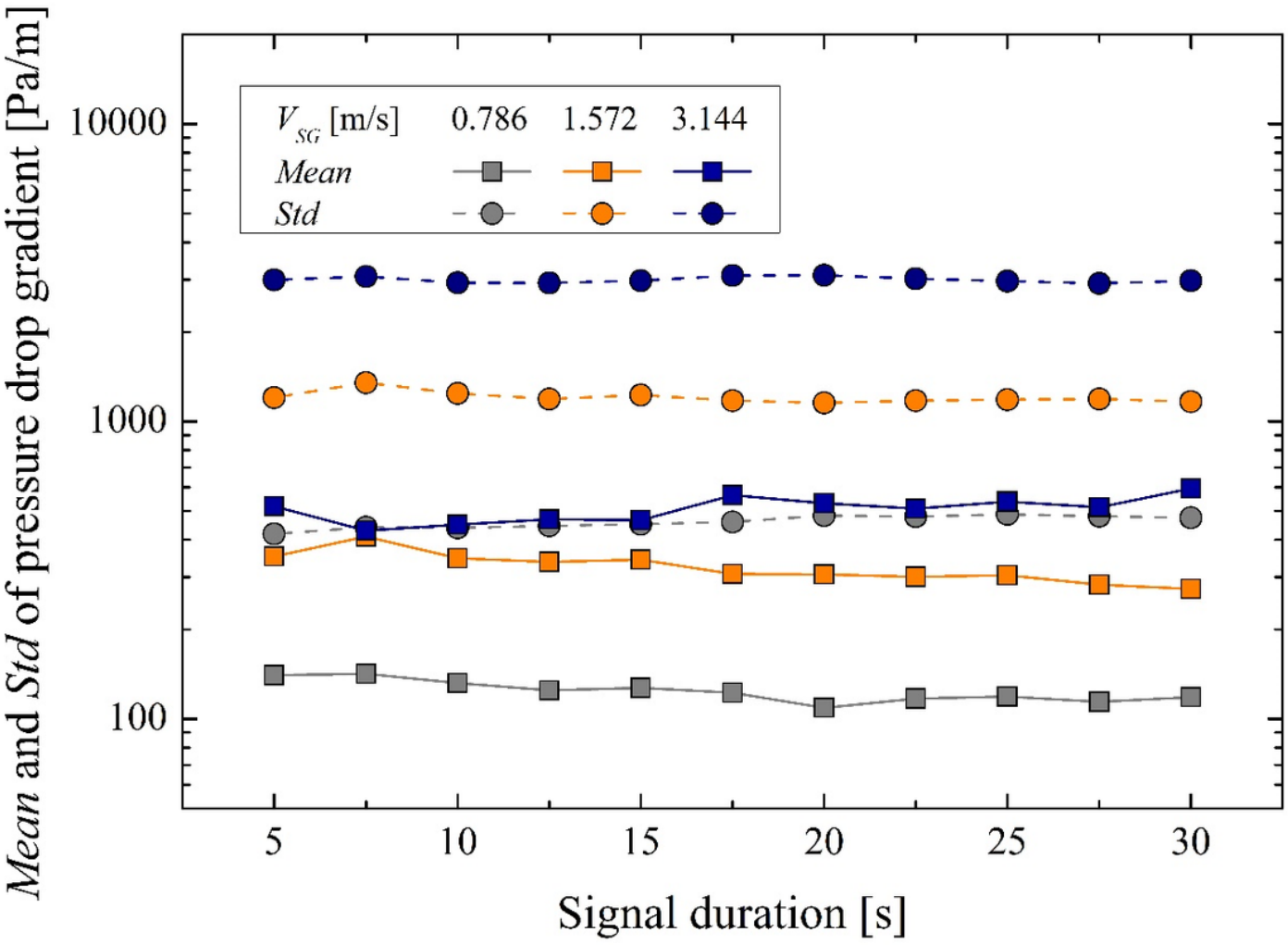

Figure 3

Influence of the sampling duration on mean and standard deviation of the pressure drop gradient for different values of V_{SG} and V_{SL} = 0.354 m/s.

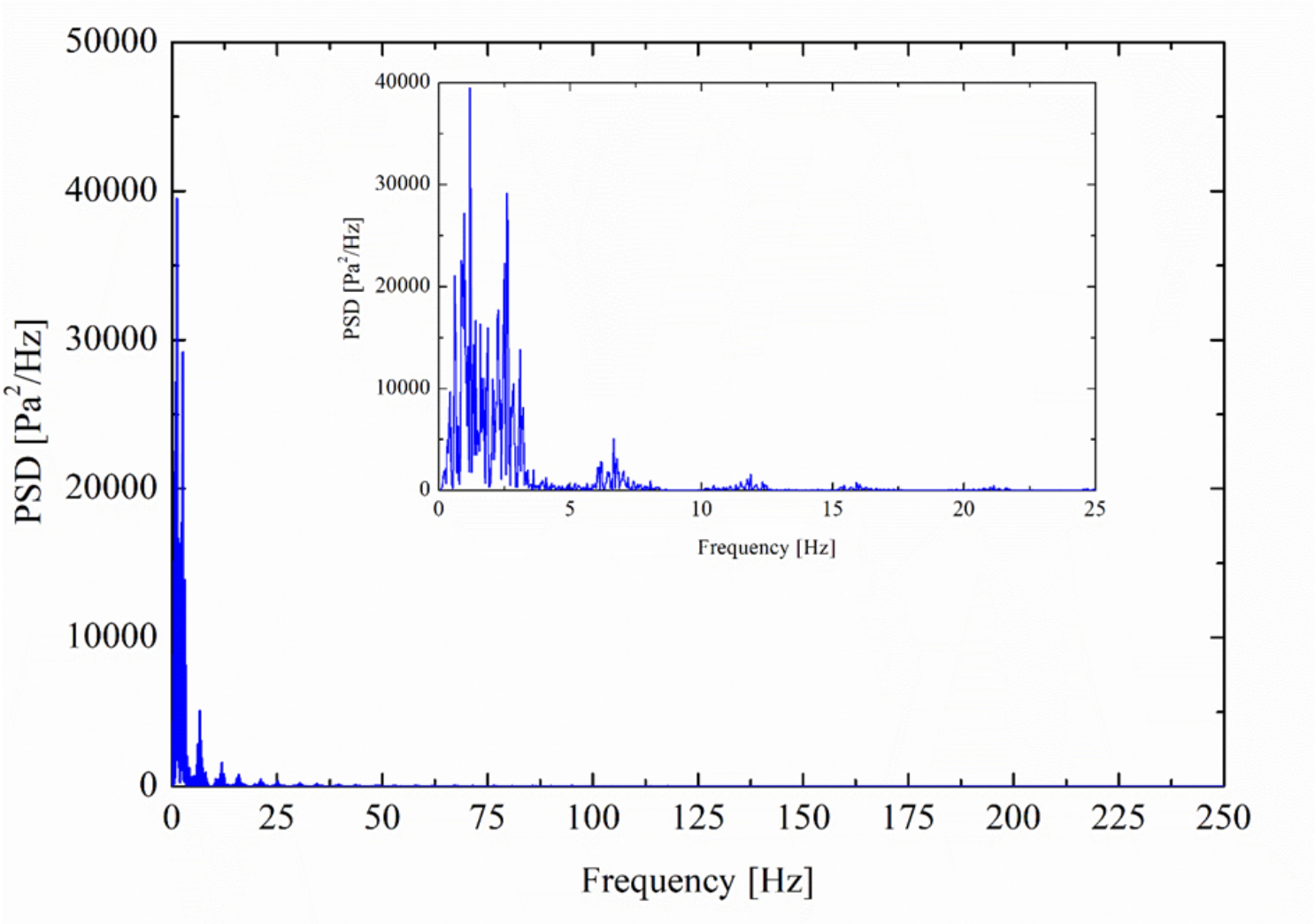

Figure 4

Example of Power Spectral Density (PSD) obtained (V_{SL} = 0.495 m/s and V_{SG} = 1.572 m/s).

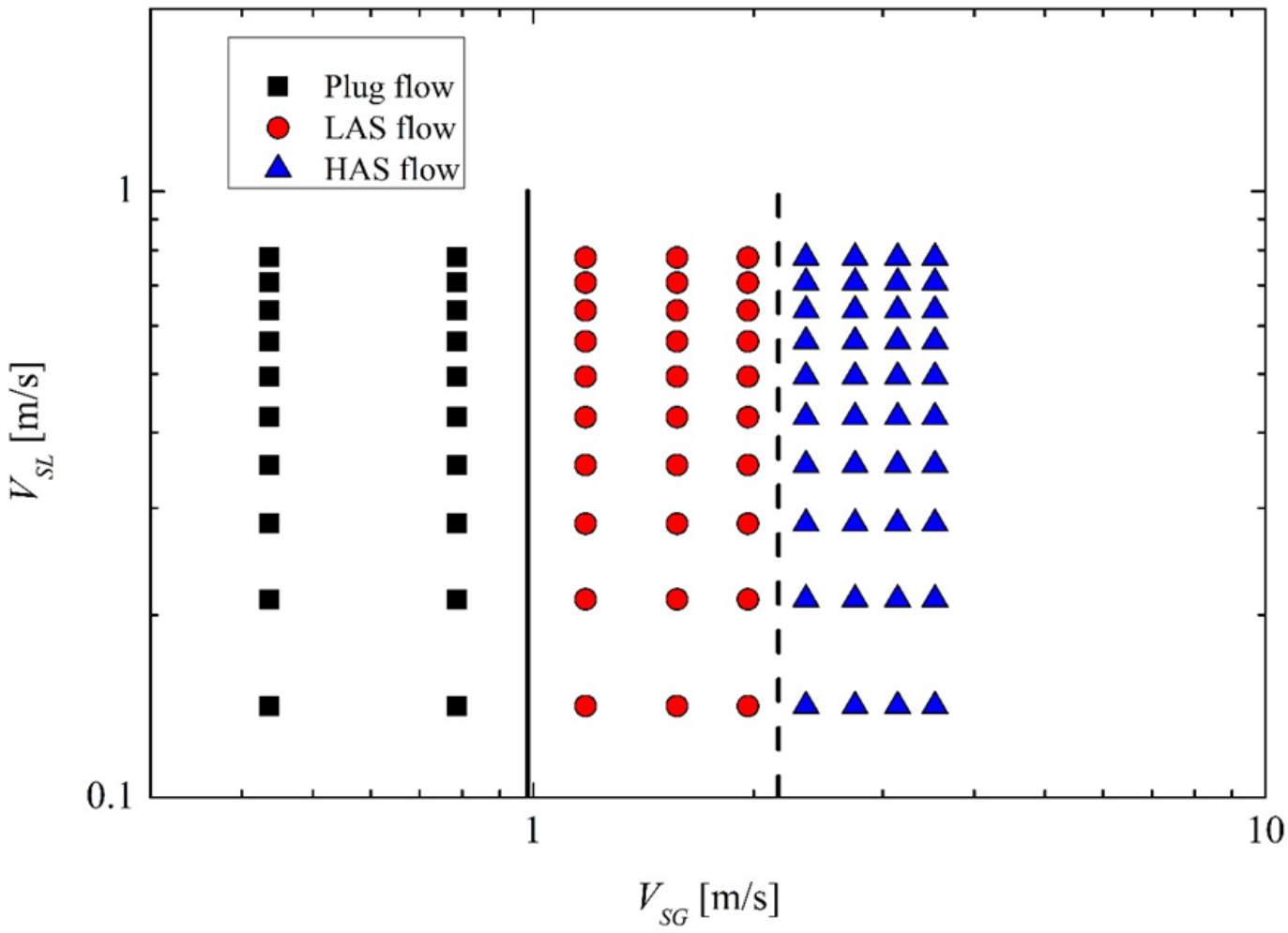

Figure 5

Plot the experimental data points of the three sub-regimes observed using V_{SL}-V_{SG} plane.

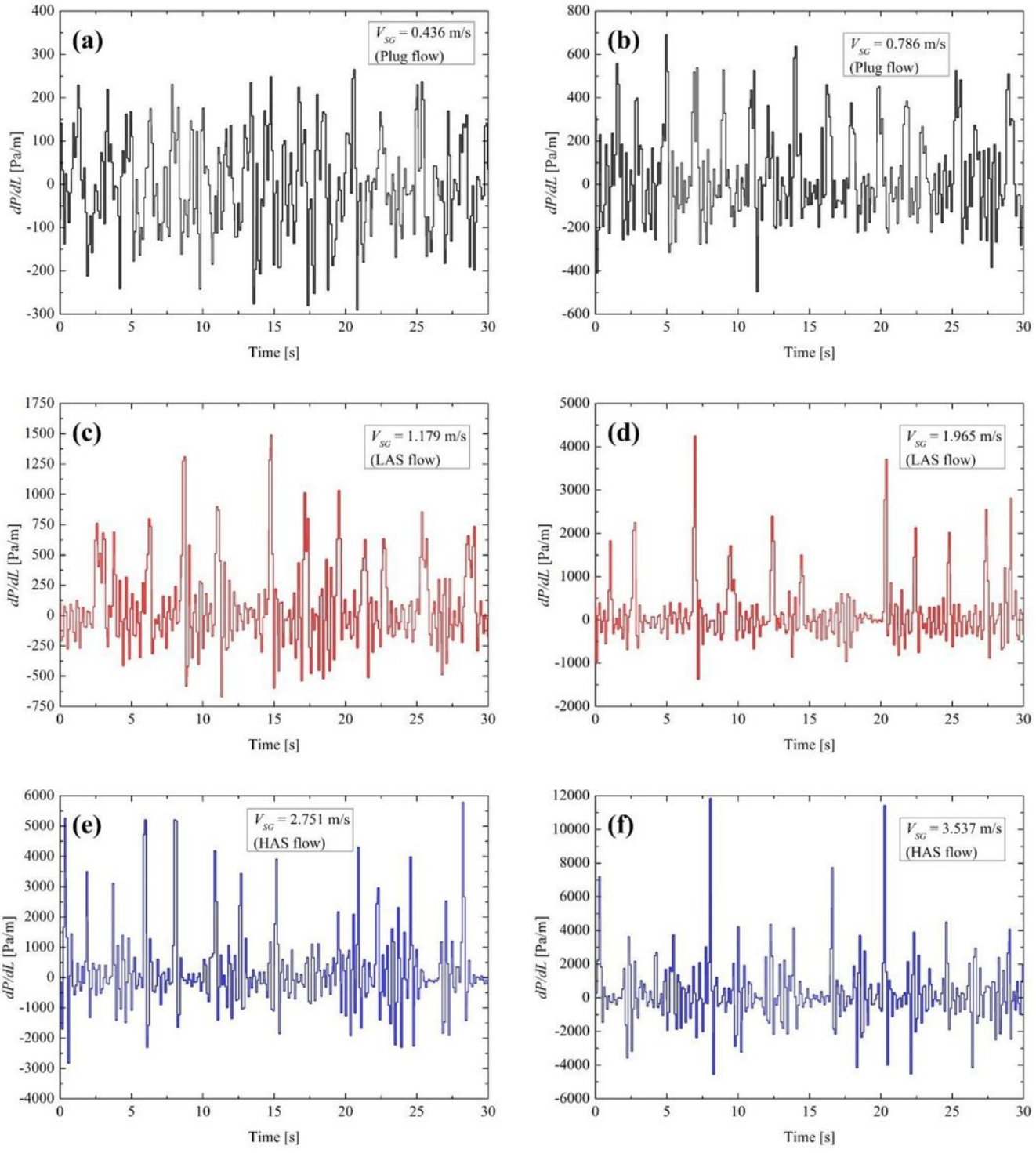

Figure 6

Examples of pressure drop gradient signal obtained for different gas superficial velocities and V_{SL} = 0.212 m/s.

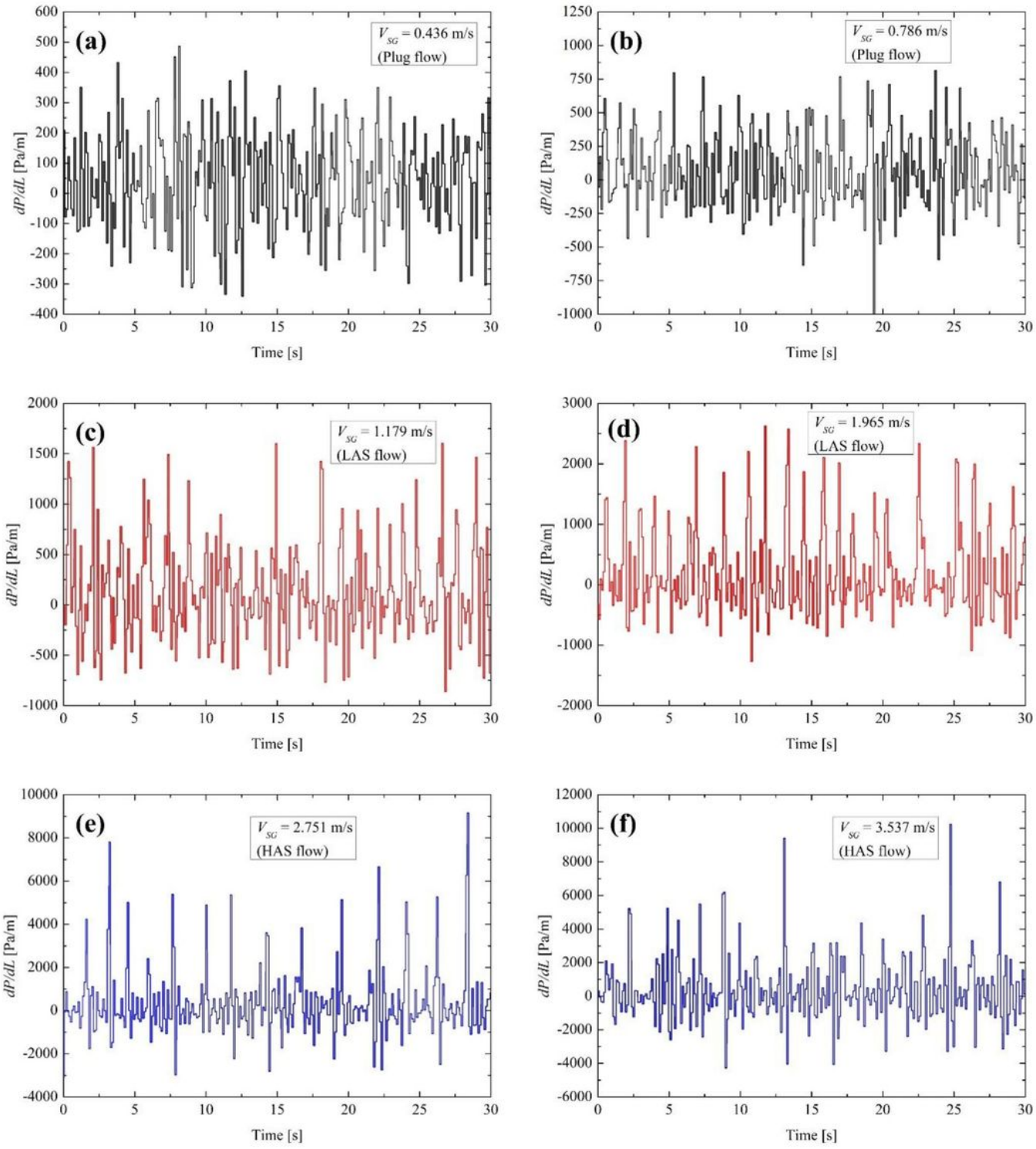

Figure 7

Examples of pressure drop gradient signal obtained for different gas superficial velocities and V_{SL} = 0.354 m/s.

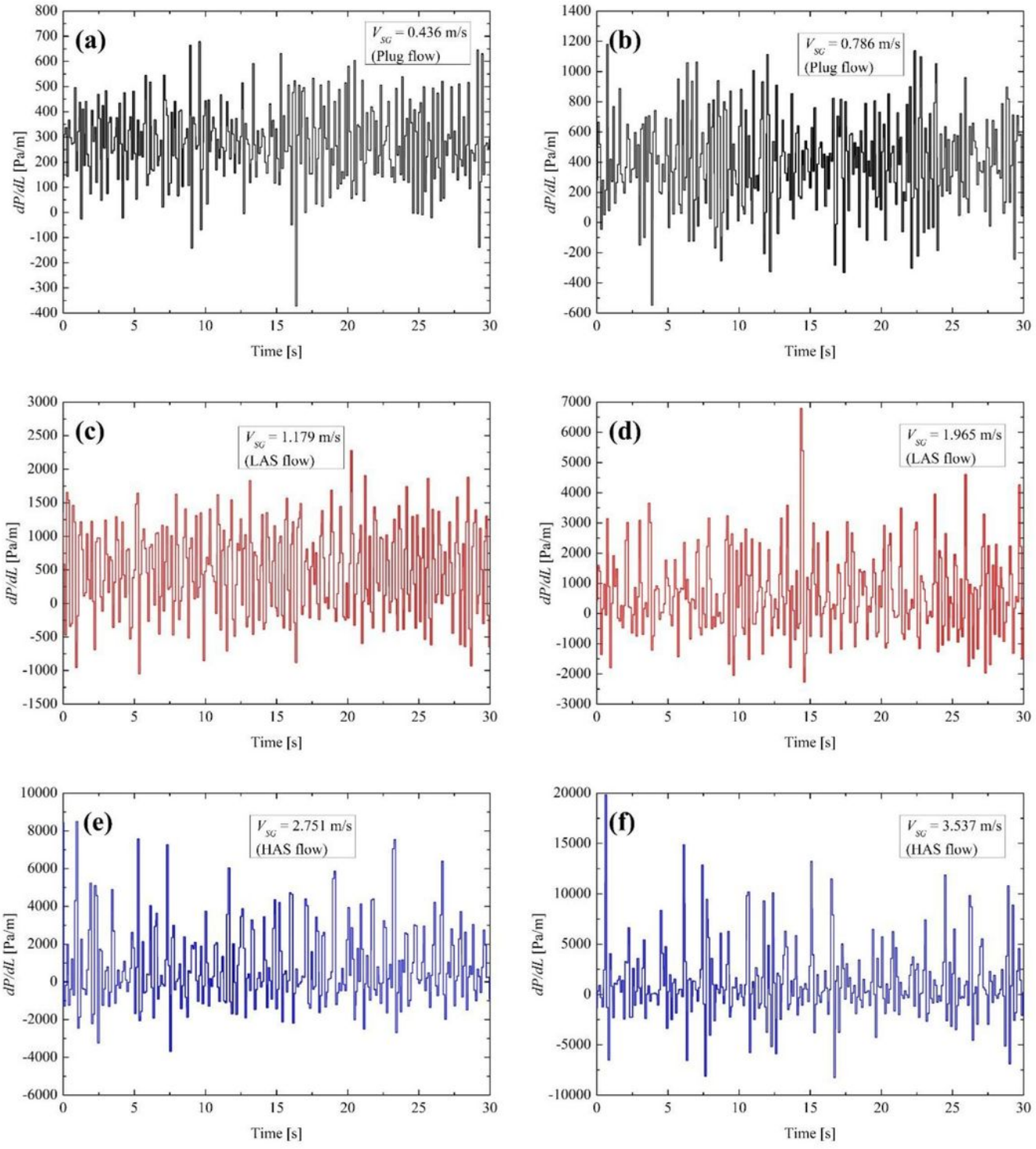

Figure 8

Examples of pressure drop gradient signal obtained for different gas superficial velocities and V_{SL} = 0.778 m/s.

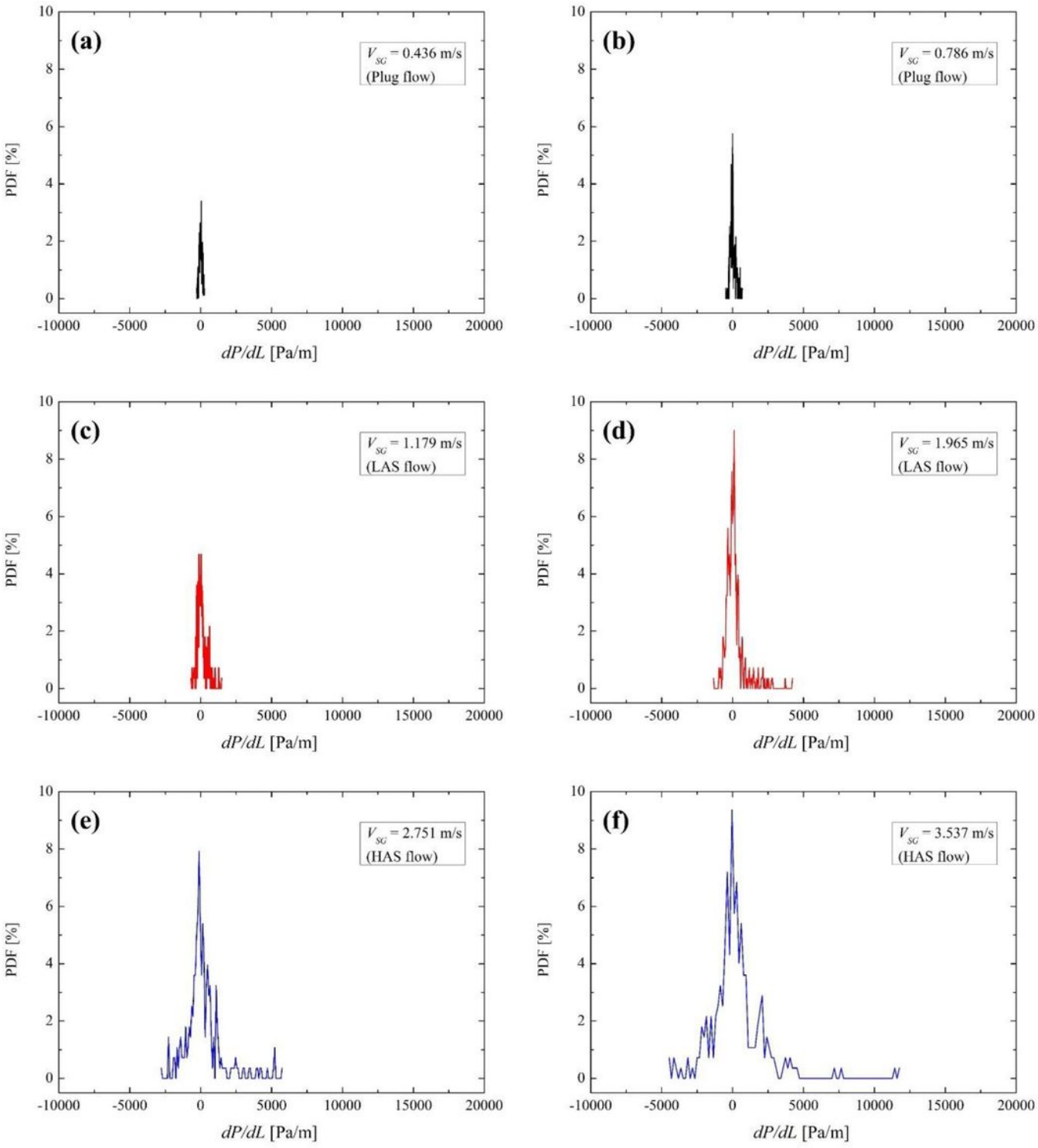

Figure 9

Examples of PDF obtained for different gas superficial velocities and V_{SL} = 0.212 m/s.

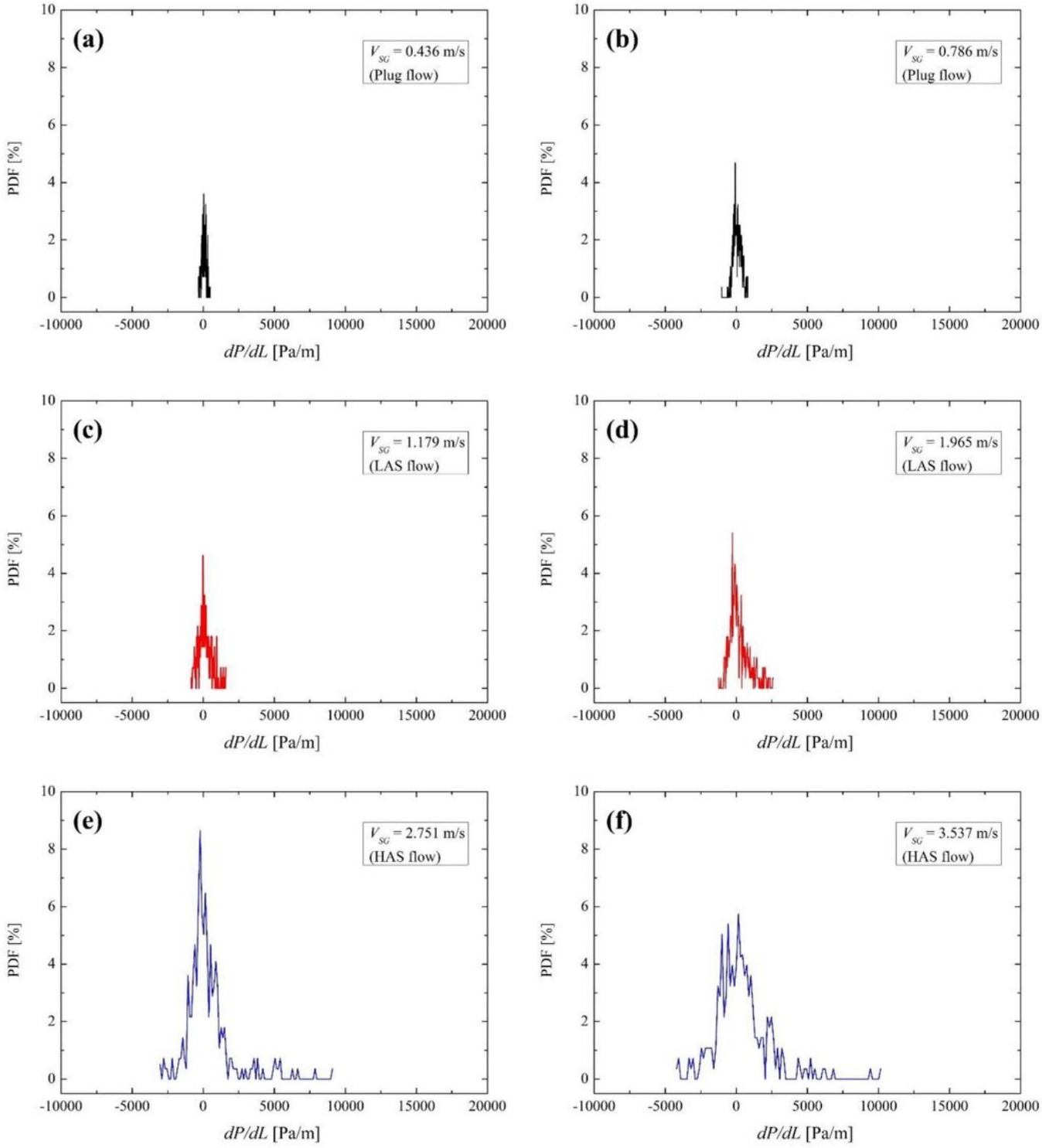

Figure 10

Examples of PDF obtained for different gas superficial velocities and V_{SL} = 0.354 m/s.

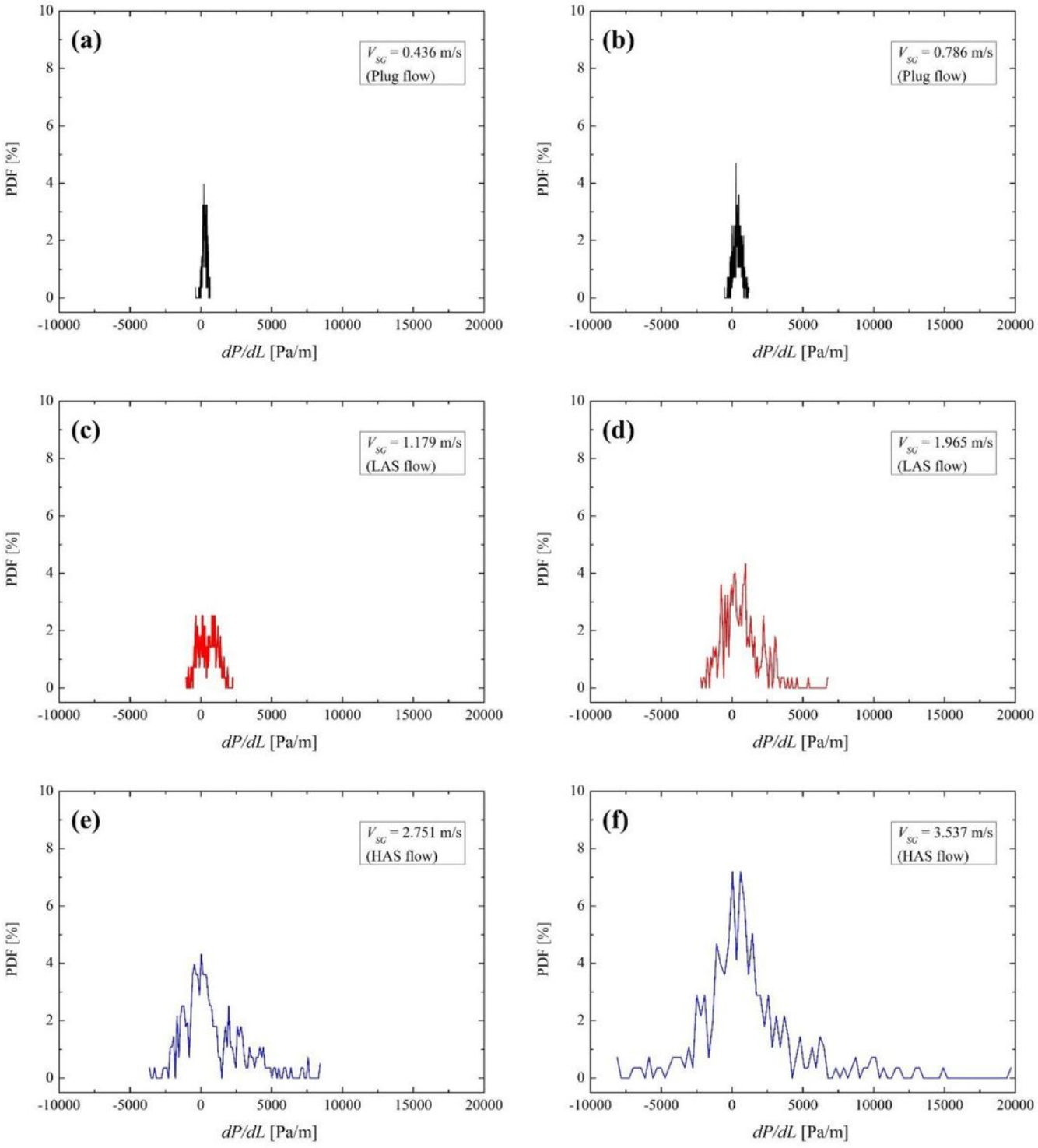

Figure 11

Examples of PDF obtained for different gas superficial velocities and V_{SL} = 0.778 m/s.

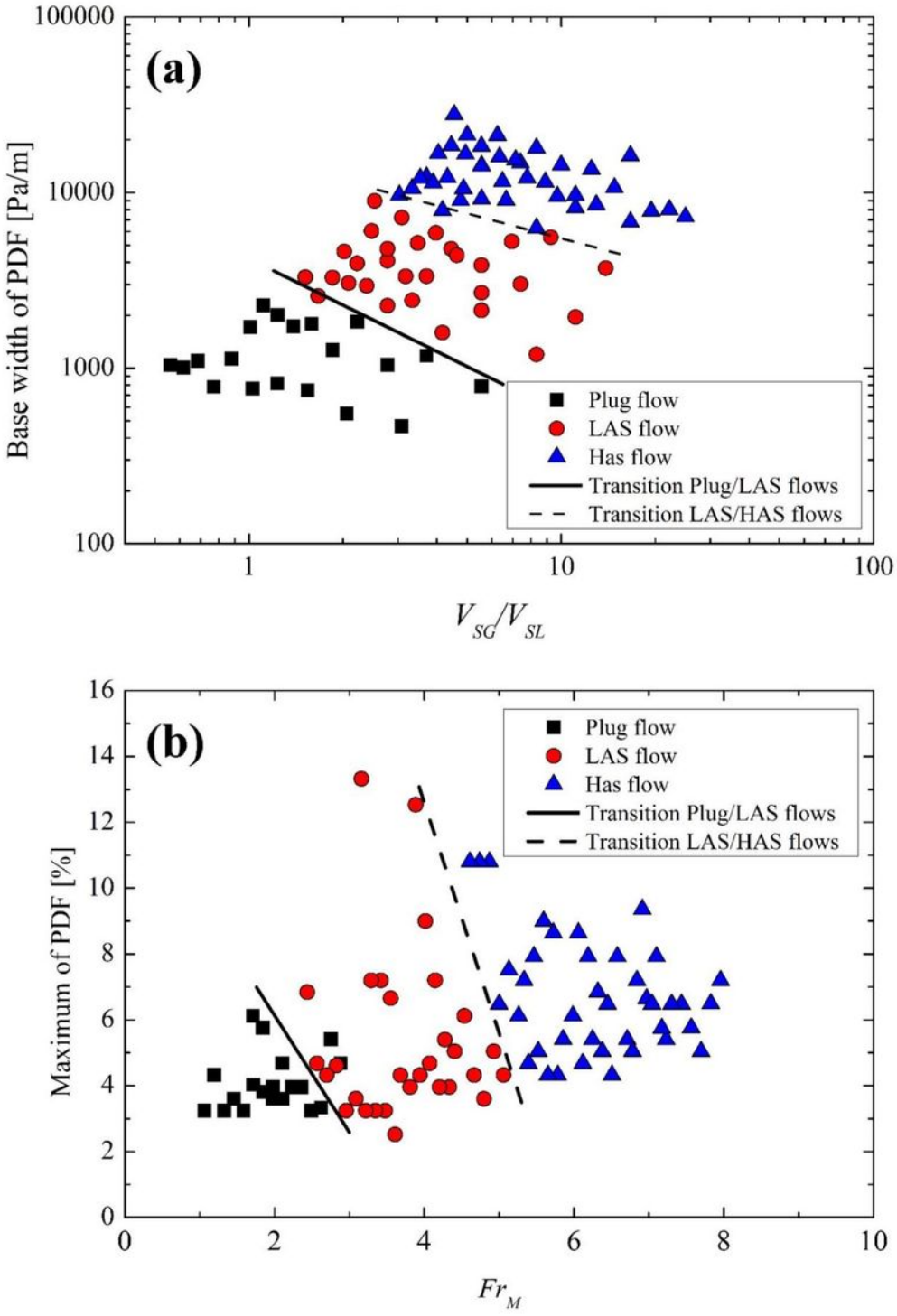

Figure 12

The plot of the data collected for each sub-regime using (a) Base width of PDF in function of the gas-to-liquid superficial velocities ratio (V_{SG}/V_{SL}) and (b) Maximum values of PDF against mixture Froude number (Fr_M).

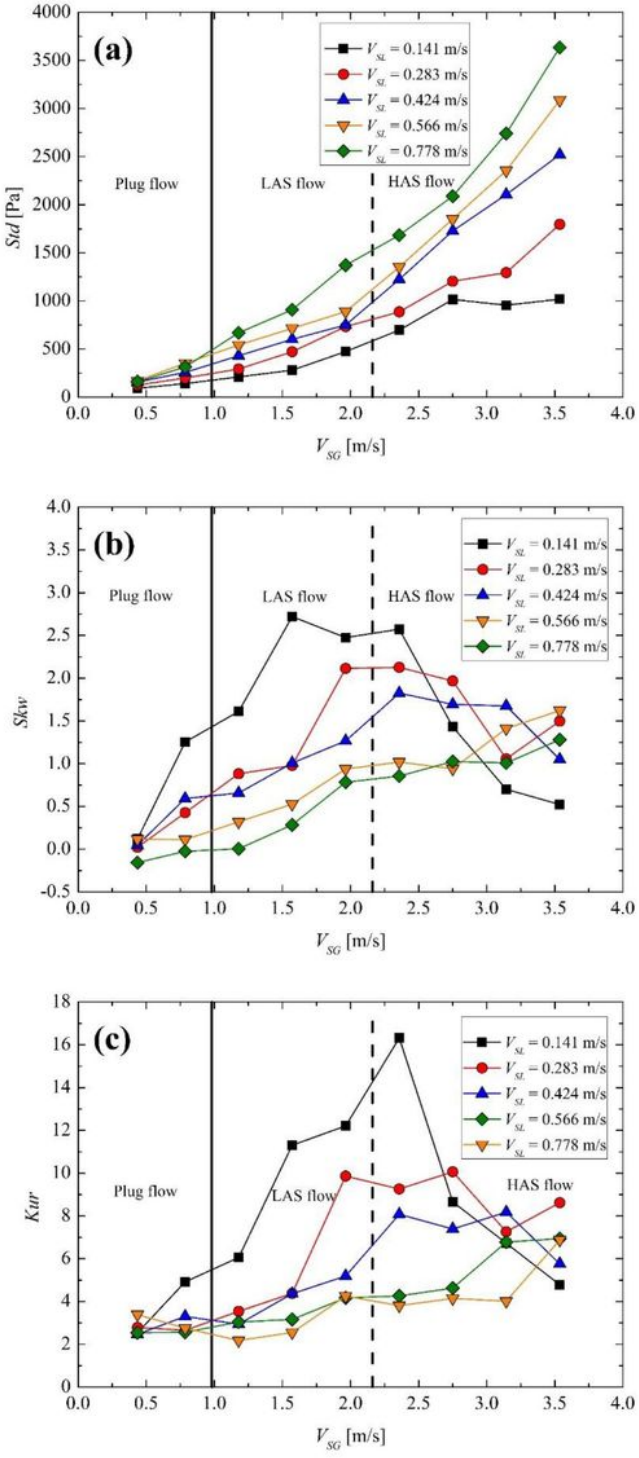

Figure 13

Influence of V_{SG} on (a) standard deviation; (b) skewness and (c) kurtosis.

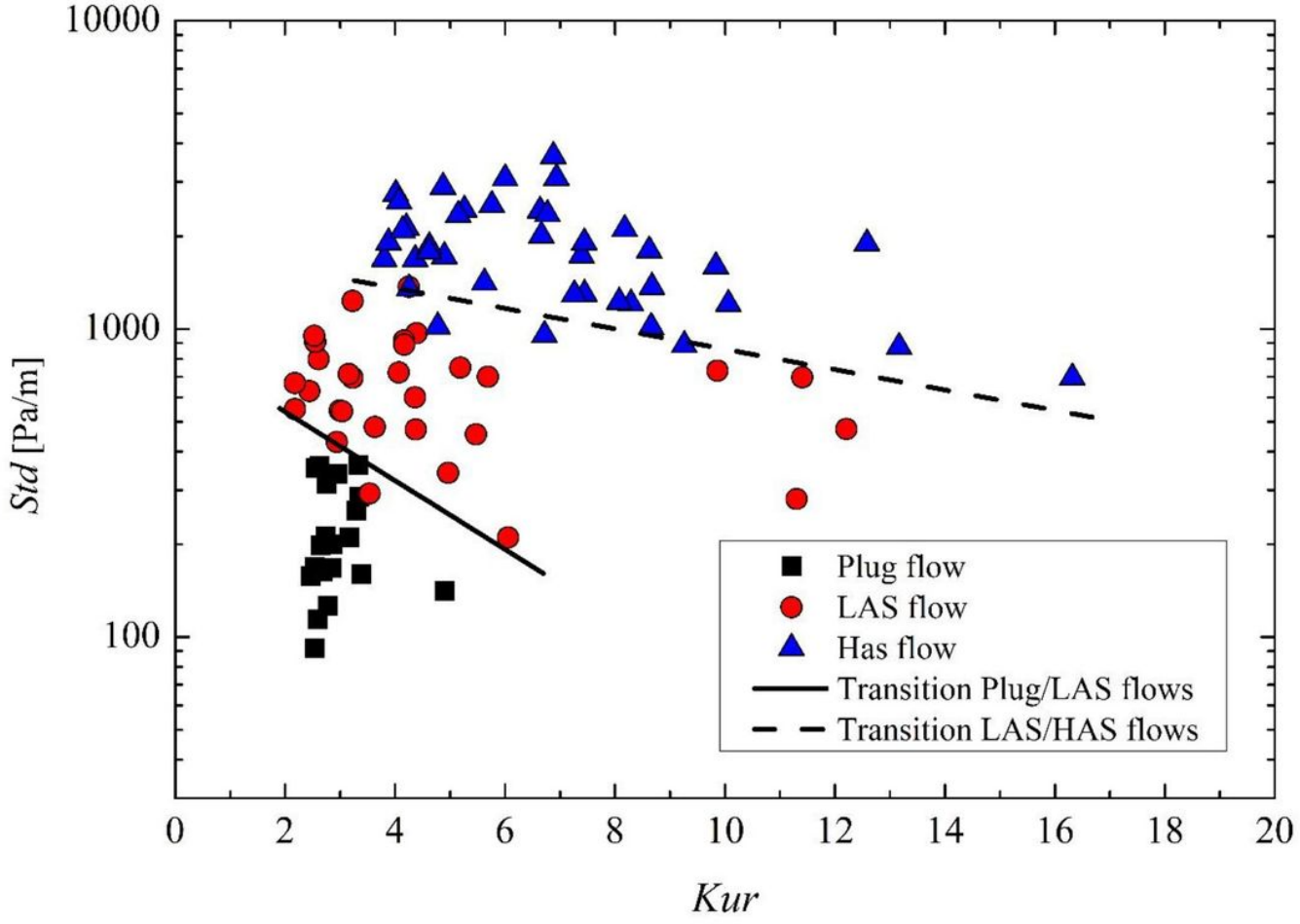

Figure 14

The plot of the data collected for each sub-regime using standard deviation in function of the kurtosis.

Supplementary Files

This is a list of supplementary files associated with this preprint. Click to download.

- Appendix.docx